Position-sensitive device

Bodo Kaiser

Ludwig-Maximilians-Universität München

bodo.kaiser@physik.uni-muenchen.de

October 5, 2020

Contents

1. Introduction

We define a position-sensitive device as a device that outputs voltages proportional to the center of mass coordinates of a light beam incident on a sensitive area.

The present document summarizes the insights acquired on the journey of building such a device.

1.1. Motivation

Position-sensitive devices are used in a wide range of industrial and commercial applications, including displacement sensing and beam alignment, see Ref. [**Maekynen00**].

We are interested in using a position-sensitive device for beam pointing alignment in our quantum optics laboratory.

The beam pointing refers to a laser beam's spatial focus and can change through thermal and mechanical effects. Uncompensated changes in beam alignment can quickly degrade the overall performance of an optical system. Therefore, it is crucial to align the beam pointing to ensure the optical system's proper operation at hand.

1.2. Overview

This document is organized as follows. The first section discusses the details of the electrical schematic and should be used as a reference to adjust parameters. The second, third, and fourth sections are relevant for the assembly of the position-sensitive device. The last section discusses the testing procedures for quality control. The appendix contains more details, including references, about the theory of the (position-sensitive) photodiode and operational amplifiers.

1.3. Requirements

The requirements are specified rather loose. The only hard requirement concerns the connectors and voltages of the power supply. The power connector should be a LEMO4 whose pin configuration is compatible with the 15V dual-voltage power supplies used in the labs. Features that would be nice to have are:

1. The device should be sensible with optical powers that are safe to operate, i.e., P ¡ 1 uW. There is no preferred wavelength.

2. For easy integration into existing optical setups, the device should be as compact as possible. Additional space, if needed, should be occupied by elonging the height. The sensitive area of the detector should be on the bottom. The connectors should be on the top to avoid cables blocking the beam path.

3. It should be possible to mount different detector sizes on the device.

The range of the output voltages of the device can be chosen for the optimal signal-to-noise ratio.

1.4. Specification

2. Schematic

The present section discusses the critical sections of the electrical schematics and should be consulted for reference if parameters, for example, bandwidth or gain, need to be adjusted.

2.1. Photodiode frontend

The photodiode frontend is responsible for converting the photocurrent to a voltage. The most simple frontend, a resistor, has limited bandwidth. Using a transimpedance amplifier, we can decouple the output voltage from the voltage swing across the diode. The bandwidth is now limited by the amplifier gain.

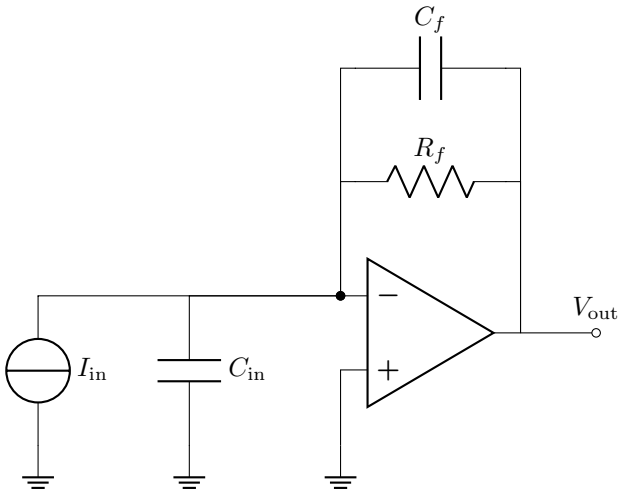

Figure 1: Transimpedance amplifier for photodiode

Figure 1 shows a transimpedance amplifier frontend circuit representing the photodiode by a current source with capacitance. The current source relates to the power of the incident light by

$$I_{\text{in}} = S(\lambda)P, \tag{1}$$

wherein $S(\lambda)$ is the spectral responsivity, also known as photosensitivity, and P is the power of the light beam. The photodiode's datasheet specifies the capacitance C_{in}.

The operational amplifier's output voltage in the transimpedance configuration is equal to

$$V_{\text{out}} = -R_f I_{\text{in}}. \tag{2}$$

A feedback capacitance

$$C_f \geq \sqrt{\frac{C_{\text{in}}}{2\pi R_f f_u}}, \tag{3}$$

wherein f_u is the gain-bandwidth-product (GBP) of the operational amplifier, is sufficient for stability. In general, the input capacitance of the operational amplifier adds to the input capacitance. In practice, solder joints and printed circuit board (PCB) traces may add to the capacitance such that a slightly higher value than given by (3) is recommended. However, if the feedback capacitance is too high, we remove high-frequency components of our signal, which might be of interest.

2.2. Voltage regulator

We use two voltage regulators to maintain a constant voltage of $\pm 12\,\text{V}$ from the external $\pm 15\,\text{V}$ power supply. The $\pm 12\,\text{V}$ voltage powers most components except the transimpedance amplifiers of the detector. Using a dedicated pair of voltage regulators to power the transimpedance amplifiers decreases the load on the primary voltage regulator.

Figure 2 shows the circuitry of the primary voltage regulators that output $\pm 12\,\text{V}$. The positive voltage regulator U1 of type LM317 and the negative voltage regulator U2 of type LM337 have an internal reference voltage of $1.25\,\text{V}$.

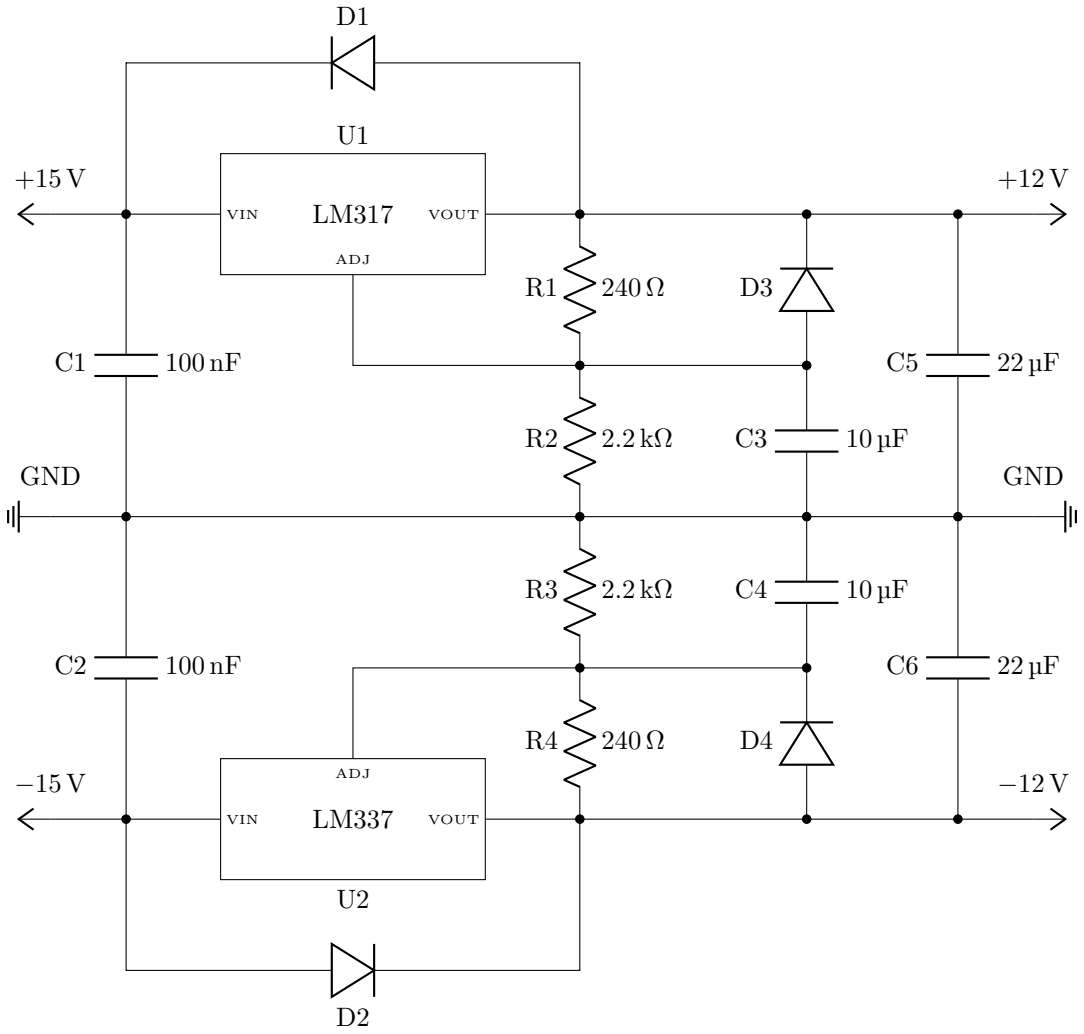

Figure 2: Dual supply voltage regulator

The voltage divider comprising R1 and R2 fixes the output voltage according to

$$V_{\text{out}} = 1.25\,\text{V}\left(1 + \frac{R_2}{R_1}\right). \tag{4}$$

With $R1 = 240\,\Omega$ and $R2 = 2.2\,\text{k}\Omega$, the output voltage is about 12.7 V, which leaves enough space for potential voltage drops in, for example, the operational amplifiers.

Diodes D1 and D3 ensure that the capacitors C3 and C5 can discharge over the external power supply.

The application notes of one of the voltage regulator's datasheets describe the presented

design. That is also the reason for not using fixed voltage regulators in this case.

2.3. Voltage reference

Reverse biasing the photodiode decreases it's capacitance and thereby increases the bandwidth. The reverse bias voltage needs to be well controlled not to cause any side-effects. Therefore, we utilize a voltage reference to supply a highly-regulated reverse voltage for the photodiode.

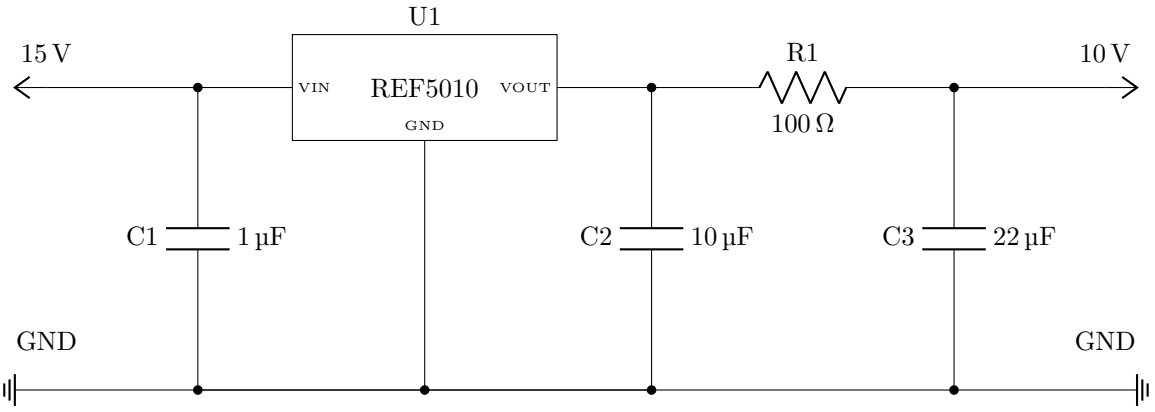

Figure 3: Voltage reference to reverse bias the photodiode

Figure 3 shows the schematic of the reverse-bias voltage reference. The capacitors C1 and C3 intercept voltage fluctuations. Resistor R1 forms a low-pass with capacitor C2 that suppresses frequencies above 160 Hz.

2.4. Analog arithmetic

Finally, we need to add and subtract the four different voltage signals of the position-sensitive photodiode to obtain quantities proportional to the incident light beam's center-of-mass. We achieve immutability of the input signals for addition and subtraction with the summing amplifier. We extend the summing amplifier to allow negative signs, i.e., subtraction.

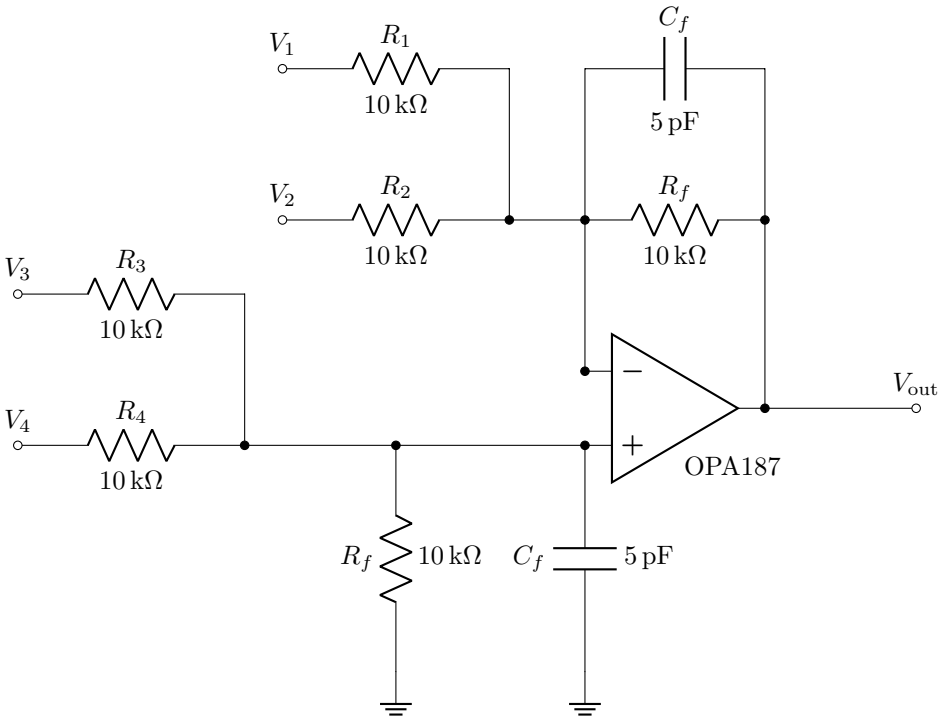

Figure 4: Summing and difference amplifier

Figure 4 shows such an arithmetic amplifier. According to [**Tietze15**] the output voltage is given by

$$V_{\text{out}} = -\frac{R_1}{R_f}V_1 - \frac{R_2}{R_f}V_2 + \frac{R_3}{R_f}V_3 + \frac{R_4}{R_f}V_4. \tag{5}$$

It is an excellent directive to have a well-controlled the bandwidth. On this account, we include capacitor C_f to control the frequency response of the amplifier. For the resistor and capacitor configuration used in fig. 4, the bandwidth is equal to

$$\frac{1}{2\pi R_f C_f} \approx 3\,\text{MHz}, \tag{6}$$

magnitudes more than the bandwidth of our transimpedance amplifiers. We place an additional capacitor with feedback capacitance at the non-inverting input of the operational amplifier to obtain a symmetric frequency response for the positive terms in (5).

The value of the resistors is 10 kΩ to limit the current flow.

3. Production

The production of the position-sensitive device involves the necessary steps to produce the detector and arithmetic PCB.

It's best to first do the arithmetic board and if it works, proceed with the detector. Of course, if you only need one of the boards, perform the following steps only once.

3.1. Commissioning

Before we can assemble the PCBs, we need to gather the required components and order missing pieces.

The list of the required components is usually known as the bill of materials (BOM). You can generate a current BOM directly from KiCad by using the InteractiveHtmlBom plugin. The plugin generates an hypertext markup language (HTML) file that lists the components and their respective placement on the PCB. Figure 5 shows where to find the plugin in the PCB editor menu. You can check if the parts are stocked and placed.

Figure 5: Menu entry for the InteraciveHtmlBom plugin for KiCad

Figure 6 and fig. 7 show the view of the generated HTML for the arithmetic and detector board.

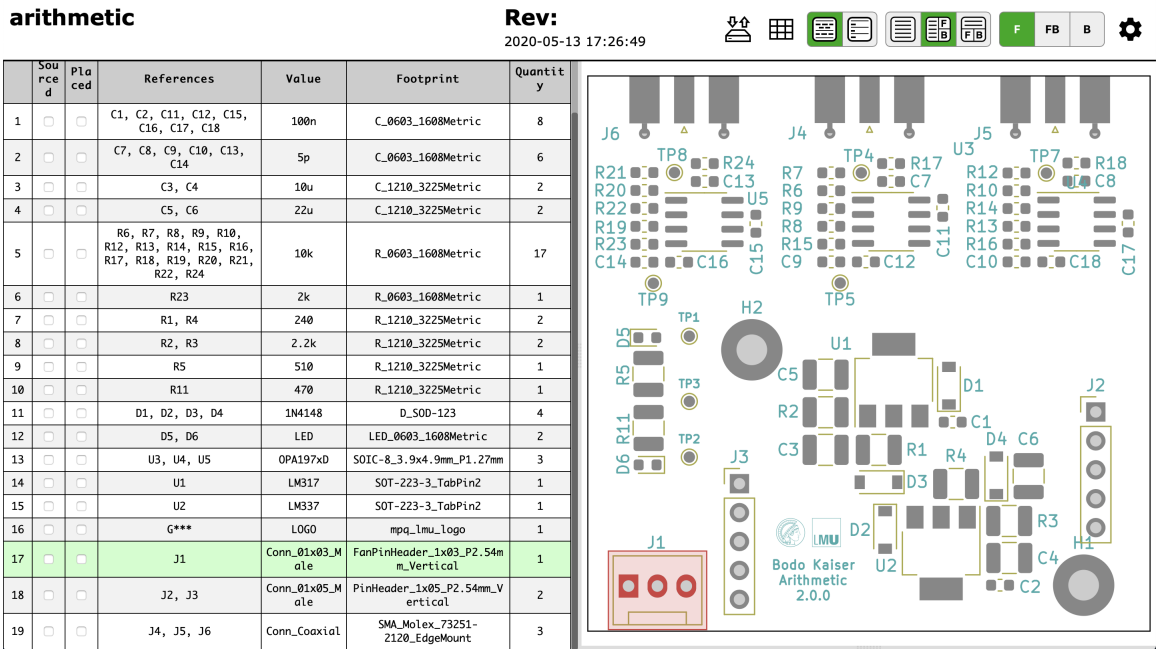

Figure 6: Arithmetic board view of the InteraciveHtmlBom plugin

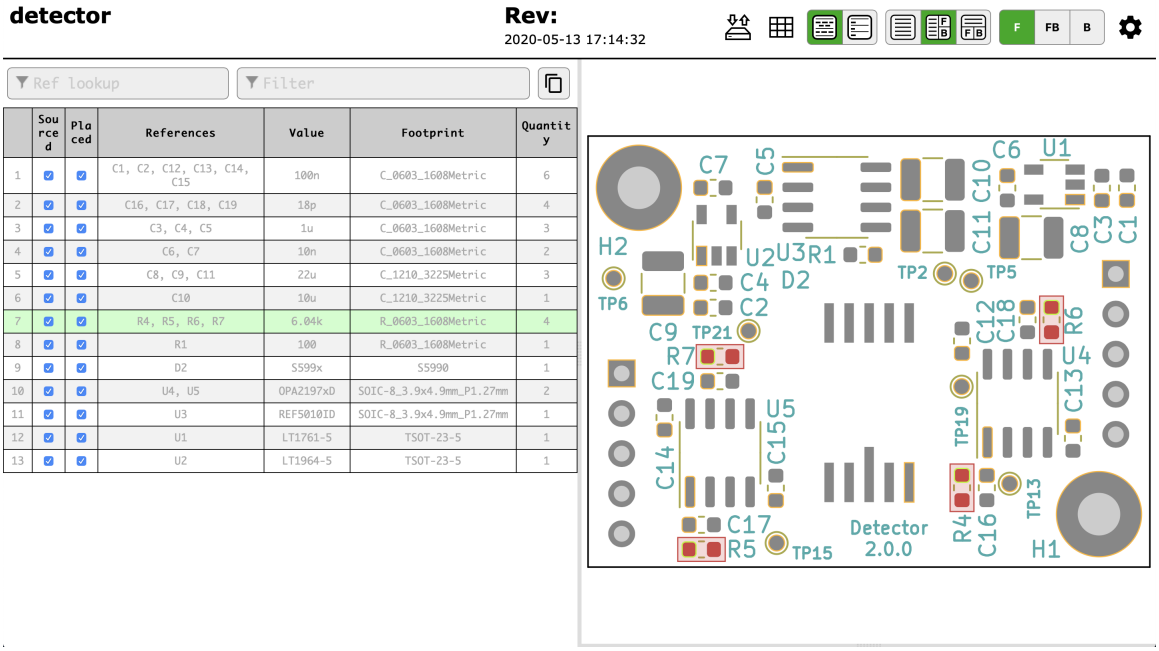

Figure 7: Detector board view of the InteraciveHtmlBom plugin

Start by checking the local inventory for the components listed by the generated HTML

BOM. If certain elements are missing, you can check the `BOM.xlsx` file inside the project repository. It contains part numbers and product links from major electronic distributors. If you order, double-check with the generated HTML BOM. There might be errors, e.g., wrong casing sizes in the `BOM.xlsx` as it is potentially outdated.

3.2. Manufacturing

In the manufacturing process, we solder the components onto the PCB. We recommend to proceed in the following steps:

1. Put on rubber gloves as the solder paste is potentially hazardous.
2. Take out the solder paste from the fridge and let it reach room temperature[1].
3. Place the solder paste onto the contacts of the PCB[2].
4. Place the surface mounted device (SMD) components onto the solder with a tweezer[3].
5. Start the oven and adjust the frame on which you place the board with the screw to the appropriate size. Use an empty PCB for this.
6. Select the profile SMD180 and follow the instructions of the oven.
7. Inspect the board for misplaced components and unmelted solder, and fix them by hand soldering[4].
8. Perform electrical testing as described in the next section.
9. Solder remaining components, for example, the SubMiniature version A (SMA) mounts or the pin headers, by hand.

[1] It is possible to use the cold solder paste directly, but it makes the handling more difficult as the paste is less fluid.

[2] Generally speaking, it is better to have too much solder paste then too less. If there is a small overlap between the contacts, this is fine as the solder will shrink when transitioning to a liquid phase in the oven.

[3] Start with the larger components and then progress to the smaller ones

[4] You can use the solder heat gun to melt the remaining solder paste or remove misplaced components. However, you might blow away small capacitors.

3.3. Electrical testing

With the electrical testing, we want to confirm that the solder connections and components work as expected. The most basic check is that the supply voltages are correct. More elaborated checks concern the operational amplifiers but are out of the scope of this document.

For the arithmetic perform the following checks in the given order. Skipping steps might lead to permanent damage!

- ☐ Leave the arithmetic board unpowered and check for high resistance between the supply lines through the test points TP1 (12 V), TP2 (GND), and TP3 (−12 V)[5].
- ☐ Configure the power supply to provide a dual voltage of ±15 V[6]. If possible, limit the current of the voltage sources.
- ☐ Confirm that the output voltages are correct with the multimeter.
- ☐ Connect the power supply with the arithmetic board but double-check the polarity.
- ☐ The voltage between TP2 and TP1 should read around 12 V while the voltage between TP2 and TP3 should read about −12 V.
- ☐ Confirm that the supply voltages reach the op-amps.
- ☐ Check the temperature of the integrated circuit (IC)s. If any IC is very hot, there is a short.
- ☐ Check if the op-amps work by grounding the inverting input and confirming that the output voltage changes to 0 V.

For the detector perform the following checks in the given order. Skipping steps might lead to permanent damage!

- ☐ Leave the detector board unplugged and confirm high resistance between GND (you can use the middle pin of the headers), TP5 (5 V), and TP6 (−5 V).
- ☐ Confirm a change of the voltage between the photodiode and GND's outer pins while illuminating the sensitive area of the photodiode with a laser pointer.

[5] If there is low resistance (> 10 kΩ), you probably have a short through soldering.

[6] Alternatively, use two single voltage sources set to 15 V and connect the negative port of one of the voltage sources with the other one's positive voltage.

- ☐ Mount the detector board on the arithmetic board, and measure the detector board's supply voltages.

- ☐ Confirm that the voltage reference (U3) outputs 10 V and that the op-amps have the correct supply voltage of ±5 V.

Finally, we test the arithmetic amplifiers on the arithmetic board.

- ☐ Mount the detector onto the arithmetic board.

- ☐ Measure the voltage at the outputs of the operational amplifiers of the arithmetic board. For the summing amplifier (U5), we expect an increase in voltage when illuminating the photodiode with the laser pointer. For the difference amplifiers (U3, U4), we expect the voltage to change when moving the laser pointer's focal spot on the photodiode.

4. Measurement

In the present section, we will perform some measurements with the position-sensitive detector (PSD). In particular, we want to determine the spatial resolution and discuss the noise characteristics.

4.1. Electrical setup

Table 1 lists the equipment required for the electrical setup. The electric devices are connected as follows. The PSD is connected with the power supply through the LEMO4 cable. The DIFFX, DIFFY, and SUM output voltages of the PSD are conencted to the oscilloscope's first three input channels. It is essential to use shielded cables to avoid receiving 50 Hz noise from surroudning switching power supplies.

Device	Amount
PSD	1
Oscilloscope	1
± 15 V voltage supply	1
Shielded LEMO4 cable	1
Shielded SMA cable	3
SMA to BNC adapters	3

Table 1: Electrical equipment required to operate the PSD

You can configure the oscilloscope to show the first two input channels in X-Y mode. In X-Y mode, the signal on the coordinate grid corresponds to the position of the incident light spot. Suppose your light source shows strong intensity fluctuations. In that case, you can use the oscilloscope's arithmetic operation to divide the DIFFX and DIFFY signals by the SUM signal.

4.2. Optical setup

Figure 8 shows an optical setup for spatial resolution measurements. The arrangement comprises a laser source, two mirrors, a lens, and the PSD. Using two mirrors instead of one allows more freedom in positioning the other optics. The lens focuses the laser beam onto the sensitive area of the PSD.

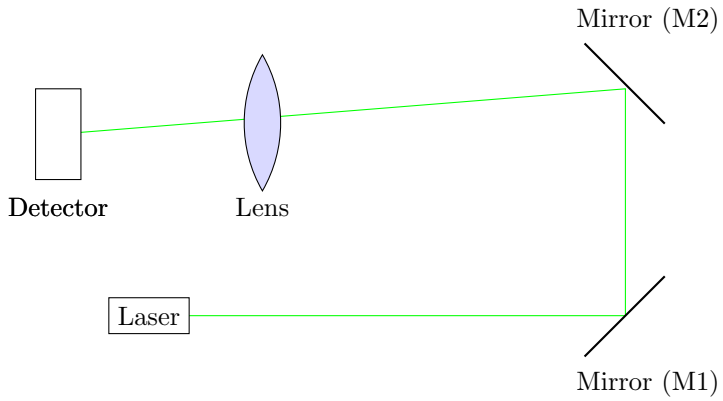

Figure 8: Optical setup for testing

4.3. Protocol

4.4. Evaluation

A. Theory of photodiode operation

A.1. Transverse photodiodes

The purpose of the following section is to recall the mechanics of the (transverse) photoeffect observed in an illuminated p-n junction. Figures and the description thereof is largely based on Ref. [**Simon13**]. A subtle difference in the depicted figures and the figures of Ref. [**Simon13**] is that we exchanged the order of p- and n-type semiconductors. We found this order to be more intuitive when referring to a p-n junction.

Figure 9 shows a separated p- and n-type semiconductor. In the upper half, we see an illustration of the p- and n-type semiconductor with their respective mobile charge carriers. The p-type semiconductor has an excess of positive charge carriers (holes) which are depicted as white circles. The n-type semiconductor has an excess of negative charge carriers (electrons) which are depicted as black circles. The excess charge carriers form due to the implantation of acceptor and donator ions. These are depicted as circles with plus and minus sign in Figure 9. The implanted ions have more or fewer electrons than the atoms of the semiconductor material. Therefore donating an electron or accepting an electron and effectively forming a hole as an absence of negative charge.

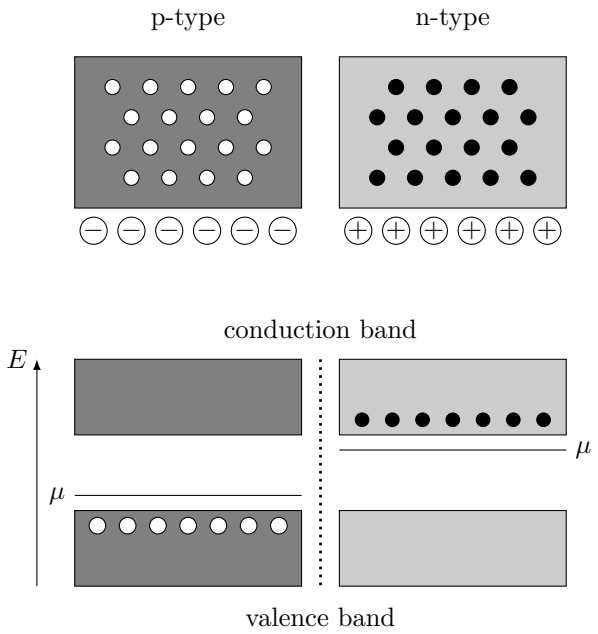

Figure 9: Separated p- and n-type semiconductor with holes (white) and electrons (black).

The lower half of Figure 9 shows the energy band structure of both p- and n-type semiconductor. The lower energy band represents the valence band made up of the electrons that are tightly bound to a single atomic core. The upper energy band represents the conduction band made up of electrons that are are not bound to a single atomic core but shared across the lattice. Charge carriers in the conduction band can move freely and thereby contribute to the conductivity of the material. For an undoped (intrinsic) semiconductor the chemical potential is in the center of the band gap between the conduction and valence band. Through doping, the chemical potential is shifted in the p- and n-type semiconductor. In the p-type semiconductor, acceptor ions can take up electrons from the conduction band, thereby decreasing the chemical potential. In the n-type semiconductor, donator ions contribute electrons to the conduction band, thereby increasing the chemical potential.

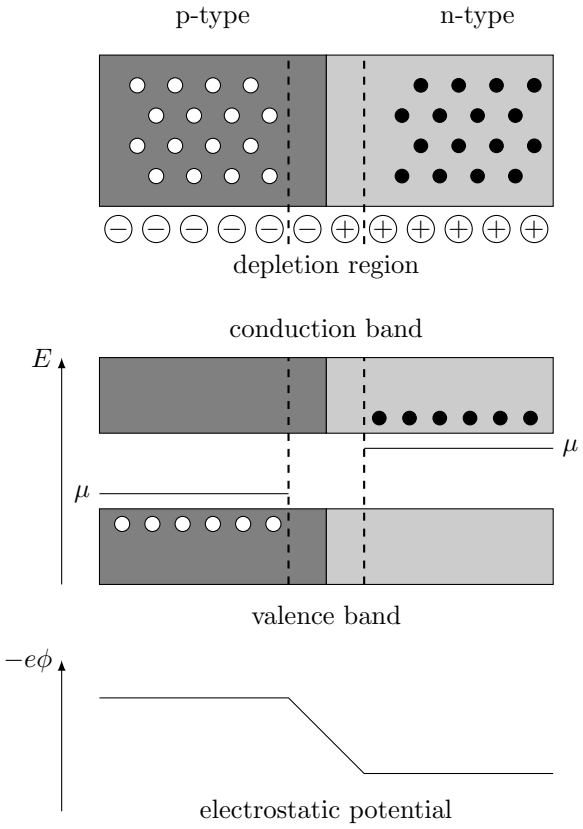

Figure 10: Combined p- and n-type semiconductor with holes (white) and electrons (black).

In Figure 10 the p- and n-type semiconductor are brought into contact with each other, forming a p-n junction. In close proximity of the junction holes and energies recombine due to a diffusion process, leaving an electrically charged area. The electrically charged

area creates an electrostatic potential across the junction as illustrated in the lower part of Figure 10. We refer to this area as the depletion region. In Figure 10 the depletion region expands between the dashed lines around the junction.

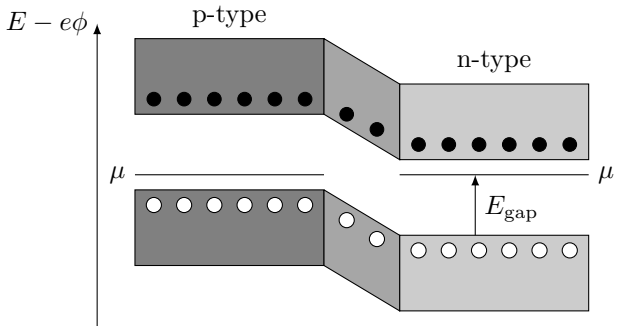

Figure 11: Energy bands of the p-n junction.

The energy band diagram in Figure 11 accounts for the shift in energy due to the electrostatic potential. The chemical potentials of both sides of the junction are now aligned. The energy required to excite an electron on the p-type side from the valence to the conduction band and the energy required to excite a hole from the conduction to the valence band are equal to the band gap of the semiconductor.

If one applies a reverse bias voltage across the p-n junction, the effective energy gap between conduction and valence band is reduced, the electrostatic potential increases and the depletion region broadens. The situation of an applied reverse voltage is depicted in Figure 12.

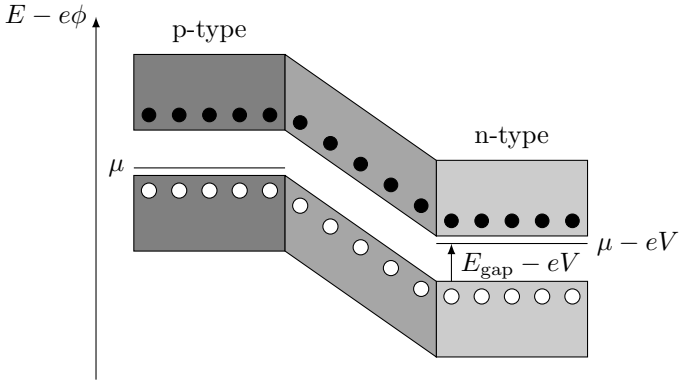

Figure 12: Energy band diagram of a reverse biased p-n junction.

The current-voltage characteristic of the p-n junction is described by the Schockley diode

equation,

$$I_{\text{diode}} = I_{\text{sat}}(T)\left(e^{eV/k_BT} - 1\right), \tag{7}$$

wherein $I_{\text{sat}} \propto e^{-E_{\text{gap}}/k_BT}$ is the temperature dependent reverse bias saturation current and V the voltage applied to the p-n junction. Using the proportionality of the reverse bias saturation current, we can write,

$$I_{\text{diode}} \propto e^{(eV-E_{\text{gap}})/k_BT} - e^{-E_{\text{gap}}/k_BT}, \tag{8}$$

which discloses the two effects contributing to the diode current. The left-hand side of the proportionality of Equation (8) represents the current contribution due intra-band excitation of charge carriers, whereas the right-hand side represents the current contribution due to inter-band excitation.

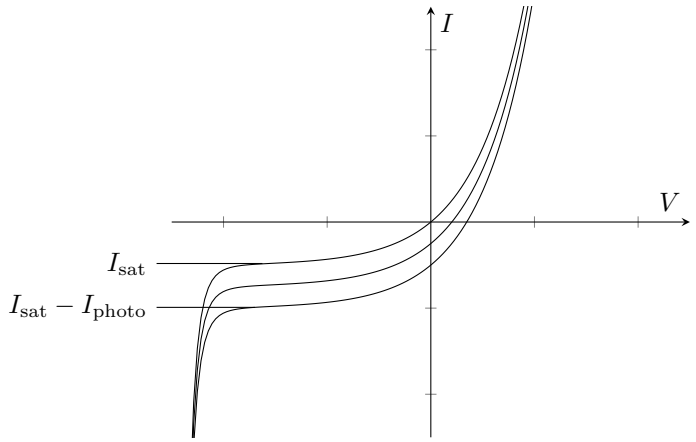

Figure 13: Current-voltage characteristics of a p-n junction with different levels of illumination.

In Figure 13 we see the current-voltage characteristics of the p-n junction under different levels of illumination. For negative voltages, the p-n junction is operated under reverse bias. If the reverse bias voltage exceeds the breakdown voltage the p-n junction starts to conduct. The current before the breakdown occurs is the reverse saturation current. For different levels of illumination, the curve is shifted downwards. The separation between the non-illuminated (top curve) and illuminated curves represent the respective photocurrent.

The conversion rate of photons to photoelectrons depends on the type of the band gap, i.e. direct or indirect, the wavelength λ of the photon and the temperature T. Most photodiodes report a wavelength λ dependent responsitivity R which can be used to convert the radiant flux P of the incident light to the generated photocurrent I_{photo},

$$I_{\text{photo}} = R(\lambda)P. \tag{9}$$

For silicon-based p-n junctions, the responsitivity $R(\lambda)$ is between $0.2\,\mathrm{A\,W^{-1}}$ at 400 nm and $0.6\,\mathrm{A\,W^{-1}}$ at 950 nm.

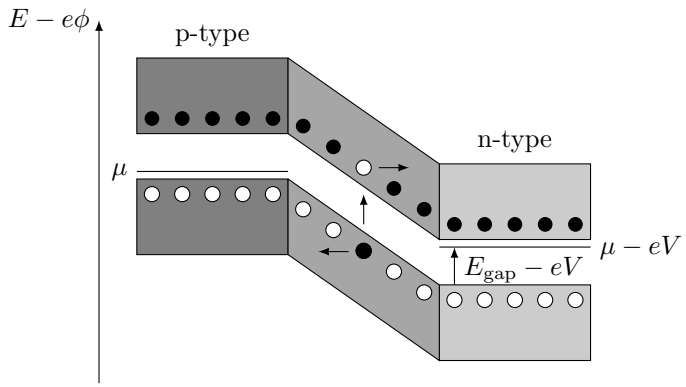

Figure 14: Energy diagram of a reverse biased p-n junction under illumination.

Figure 14 shows a p-n junction under reverse bias where a photon excites an electron-hole pair in the depletion region. Due to the electrostatic potential, the electron is accelerated to the right side. Analogue the hole is accelerated to the left side and in addition to the diode current, Equation (7), a photocurrent can be measured across the junction.

A.2. Lateral photodiodes

In the previous section, we discussed the transversal photoeffect that is usually associated with the illumination of the p-n junction. In addition to the transversal photoeffect, the lateral photoeffect was first discovered by W. Schottky [**Schottky30**] in 1930 and later rediscovered in 1957 by J. Wallmark [**Wallmark57**]. In the present section, we summarize important results from Ref. [**Noorlag74**] and Ref. [**Woltring75**] with focus on the tetralateral photodiode which is the most common commercially available design.

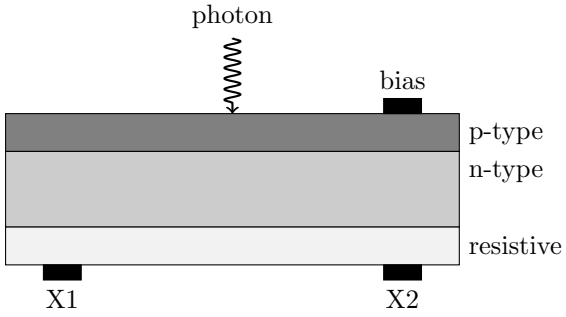

Figure 15: Cross section of a lateral photodiode.

Figure 15 depicts the cross-section of a lateral photodiode with a p-type semiconductor as the top, an n-type semiconductor as the middle layer and a resistive material as the bottom layer. An electric contact embedded into the top layer can be used as a common cathode. The common cathode can be connected to the ground or a positive voltage for reverse bias operation. In contrast to the transversal photodiode, the lateral photodiode has two anode contacts positioned at the opposite sites embedded into the resistive layer. The photocurrent measured at each of the anode contacts follows an almost linear relationship with the center-of-mass of the incident light spot. Therefore the lateral photodiode can be used to measure the spatial coordinate of an incident light spot.

The dynamics of the lateral photodiode are guided by the Lucovsky [**Lucovsky60**] equation,

$$\nabla^2 V = \frac{\rho}{w} J_s \left(e^{eV/k_B T} - 1 \right) - \frac{\rho_d}{w} J_p, \tag{10}$$

wherein V is the diode voltage, ρ is the resistance per unit length of the resistive layer, J_s is the reverse-bias saturation current and J_p is the photocurrent generated due photon induced electron-hole excitation. Equation (10) can be obtained by combination of the current density continuity equation with Ohm's law and the Schottky equation, Equation (7).

According to Ref. [**Woltring75**], operation of the lateral in fully reverse-bias has the following benefits:

1. Reduced signal loss.

2. Improved response speed and resolution.

3. Improved linearity of the position.

4. Reduced temperature dependence.

In electronic engineering literature, e.g. Ref. [**Jung05**], one is sometimes discouraged from operating a photodiode under reverse-bias for highest sensitivity as the reverse-bias increased the diode leakage (dark) current. We believe that as long as the dark current is significantly smaller than the typical photocurrent, the photodiode should always be operated in reverse-bias mode as recommended Ref. [**Noorlag74**, **Woltring75**, **Wang89**, **Hobbs11**].

Assuming a fully reverse-biased lateral photodiode, we have $eV/k_BT \ll 1$ and Equation (10) simplifies to a linear second order differential (Poisson) equation,

$$\nabla^2 V \approx -\frac{\rho}{w}\left(J_s + J_p\right), \tag{11}$$

which can be solved using variable separation and a product Ansatz. The solution of Equation (11) depends on the imposed boundary conditions. The Dirichlet boundary condition, $V = 0$, should be used if an electrical contact terminates the semiconductor, otherwise, the Neumann boundary condition, $\frac{\partial V}{\partial n} = 0$, should be assumed.

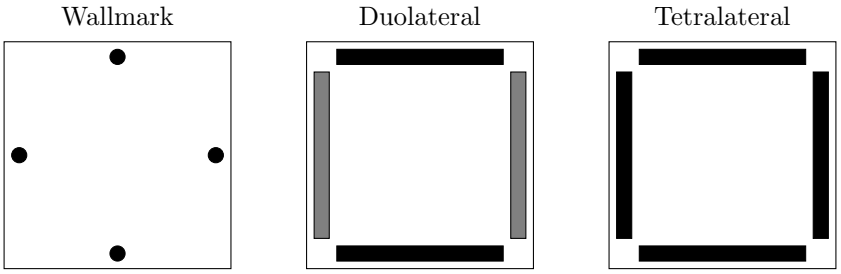

Figure 16: Contact configurations of a lateral photodiode.

In Figure 16 we present three different contact configurations. The left contact configuration was used by Wallmark [**Wallmark57**] and comprises four small electronic contacts. Assuming that the contact size is small compared to the surface of the photodiode, the von Neumann boundary condition have to be used. The middle contact configuration receives great attention from Noorlag [**Noorlag74**]. On two opposite sides of the photodiode an electric contact terminates the boundary while the remaining sides are left empty. For two-dimensional position detection, one can create two electric contacts at another layer. Mathematically we can express this configuration as combination of Neumann and Dirichlet boundary conditions. Finally, the tetralateral configuration where each side on the same layer is terminated by electric contacts can be modelled by Dirichlet boundary conditions on all sides. For a rectangular tetralateral photodiode of width l, the explicit boundary conditions are,

$$V(0, y) = V(l, y) = 0, \qquad V(x, 0) = V(x, l) = 0. \tag{12}$$

Together with the initial condition that a focused light spot hits the photodiode at

(x^*, y^*),

$$V_p(x, y, t = 0) = I_p \frac{\rho}{w} \delta(x - x^*)\delta(y - y^*), \tag{13}$$

the general solution of the Lucovsky equation, Equation (11), for the tetralateral configuration reads,

$$V_p^*(x, y) = I_p \frac{\rho}{w} \sum_{n\in\mathbb{Z}} \sum_{m\in\mathbb{Z}} \frac{\sin(m\pi x/l)\sin(m\pi x^*/l)\sin(n\pi y/l)\sin(n\pi y^*/l)}{(m^2 + n^2)\pi^2}. \tag{14}$$

The current that flows through the $x1$ contact is given by,

$$I_{x1}(x^*, y^*) = \frac{w}{\rho} \int_0^l \mathrm{d}y \left.\frac{\partial V}{\partial x}\right|_{x=0}, \tag{15}$$

respective,

$$I_{x1}(x^*, y^*) = \frac{2}{\pi} I_p \sum_{n\in\mathbb{Z}} \frac{\sin[(2n-1)\pi y^*/l]}{2n-1} \frac{\sinh[|2n-1|\pi(1 - x^*/l)]}{\sinh(|2n-1|\pi)}. \tag{16}$$

The solution does not disclose the linear relationship between anode current I_{x1} and the incident spot light coordinate x^*. Ref. [**Woltring75**] renders the non-linear distortion close to the boundaries as described by Equation (16). In order to show analytically that there is an almost linear relationship between I_{x1} and x^*, we fix $y^* = l/2$, numerically evaluate the dominant terms and Taylor expand the terms to linear order,

$$I_{x1}(x^*, l/2) = \frac{2}{\pi} I_p \sum_{n\in\mathbb{Z}} \frac{(-1)^{n+1}}{2n-1} \frac{\sinh(|2n-1|\pi(1 - x^*/l))}{\sinh(|2n-1|\pi)} \tag{17}$$

$$\approx I_p \left\{0.25 - 0.41731 \left(\frac{x}{2l} - 1\right)\right\} + \mathcal{O}\left(\left(\frac{x^*}{l} - \frac{1}{2}\right)^2\right). \tag{18}$$

Using the difference between two opposite contacts and normalizing for the total photocurrent, we find,

$$\frac{I_{x2}(x^*, l/2) - I_{x1}(x^*, l/2)}{I_{x1}(x^*, l/2) + I_{x2}(x^*, l/2)} \propto \frac{x}{l}, \tag{19}$$

which indeed is linear in x.

According to Ref. [**Noorlag74**], the tetralateral photodiode has benefits in manufacturing, although its linearity is below the duallateral photodiode, but still better than the Wallmark type, see Ref. [**Woltring75**]. Recent contact configurations have improved upon the tetralateral design in order to improve the linearity. For example, the commercially availble pin-cushion tetralateral photodiode, discussed in Ref. [**Doke87**, **Wang89**], shows good linearity over a large area. The center-of-mass of an incident light spot at (x^*, y^*) can be recovered from the anode currents via,

$$\frac{(I_{x2} + I_{y1}) - (I_{x1} + I_{y2})}{I_{x1} + I_{x2} + I_{y1} + I_{y2}} = \frac{2x^*}{l} \qquad \frac{(I_{x2} + I_{y2}) - (I_{x1} + I_{y1})}{I_{x1} + I_{x2} + I_{y1} + I_{y2}} = \frac{2y^*}{l}. \tag{20}$$

The datasheet [**HamamatsuS5990**] of the S5990, a pin-cushion tetralateral photodiode, discloses the position detectability of a light spot of size 0.2 mm over a scan interval of 0.4 mm which does not show any non-linear distortion.

A.3. Equivalent circuit

In the previous section, we described the physics behind the lateral photodiode. In the current section, we want to ignore microscopic details and concentrate on the electrical properties of real tetralateral photodiodes.

In Figure 17 the equivalent circuit of a tetralateral photodiode is depicted. The tetralateral photodiode has four anode connections X1, X2, Y1, and Y2 which are connected to the junction via position-dependent resistances R_1, R_2, R_3, and R_4. The actual junction is equivalent to two current sources I_p, I_d, a resistor R_d, and a capacitor C_d in parallel. The first current source I_p represents the generated photocurrent with typical values between µA and mA. The second current source I_d represents the generated leakage or dark current with typical values between pA and nA.

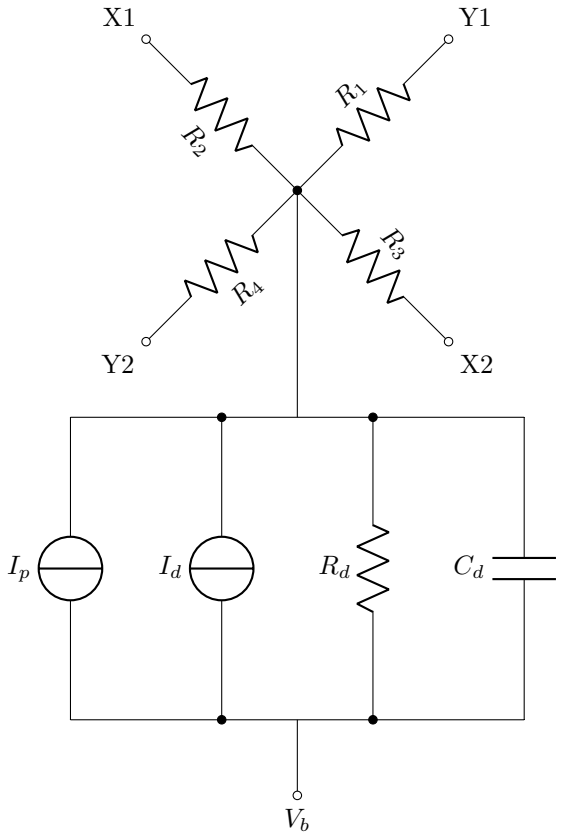

Figure 17: Equivalent circuit of a tetralateral photodiode.

The resistance R_d is referred to as interelectrode resistance and is about 10 kΩ. The capacitance C_d is also referred to as terminal capacitance and is about 150 pF. Resistance R_d and capacitance C_d form an RC pole which frequency is given by,

$$f_d = \frac{1}{2\pi R_d C_d}. \tag{21}$$

For $R_d = 10\,\mathrm{k\Omega}$ and $C_d = 100\,\mathrm{pF}$ the cut-off frequency f_d of the pole is about 1 MHz, representing the intrinsic bandwidth limit of the detector.

A.4. Signal-to-noise ratio

According to [**Woltring75**], the thermal (Johnson) noise of the resistive component of the lateral photodiode is the dominant noise source. The thermal noise is given by,

$$I_t = \sqrt{\frac{4k_B T B}{R}}, \tag{22}$$

wherein B denotes the bandwidth to consider. At room temperature $T = 300\,\mathrm{K}$ and an interelectrode resistance of $R_d = 10\,\mathrm{k\Omega}$, we find a noise current density due to thermal noise of $i_t = 2\,\mathrm{pA}/\sqrt{\mathrm{Hz}}$. If we estimate for the complete bandwidth supported by the detector we find a root-mean-squared noise current of $I_t = 2\,\mathrm{nA}$. A more realistic bandwidth incoporating later analog components would be $B = 10\,\mathrm{kHz}$, yielding $I_t = 200\,\mathrm{pA}$.

In any case, we cannot say for sure how these noise sources propagate into position detection noise. For instance, if the noise propagates in same proportions over the anodes, any error should cancel out when calculating the position. Further research has to be conducted.

B. Theory of operational amplifier

The photocurrents created by our detector are in the range of microampere where they are vulnerable to noise. Using a preamplifier, we can increase the amplitude of the signal for an improved signal-to-noise ratio. The typical photocurrent preamplifier is based on the transimpedance (current-to-voltage) amplifier design using a voltage-feedback operational amplifier. Converting the current to a voltage signal has the benefit that the voltage signal can be easily visualized with an oscilloscope. Furthermore, the voltage-feedback operational amplifier design appears to be more common than the current-feedback operational amplifier, as manufacturers offer much more choice and they are more prominent in the literature. That said, current-feedback operational amplifiers are reported to be a viable solution for high-speed and high-bandwidth applications, see Ref. [**Jung05**] for an overview of the benefits of current-feedback amplifiers and Ref. [**Carter17**] for a comparison with voltage-feedback amplifiers. An embodiment of current-feedback operational amplifiers for high-accuracy applications can be found in Ref. [**Noorlag74**].

In the following, we will always refer to the voltage-feedback operational amplifier if not noted otherwise. Moreover, we expect the reader to be familiar with the foundations of the operational amplifier. Well-written introductions to this topic can be found in [**Jung05**] and [**Carter17**].

B.1. Basic design

The basic design of a transimpedance amplifier is illustrated in Figure 18. Ignoring imperfections of the photodiode, we can represent the photodiode as a current source. The non-inverting input of the operational amplifier is connected to ground. The inverting input is coupled with the output of the operational amplifier via a feedback impedance Z_f.

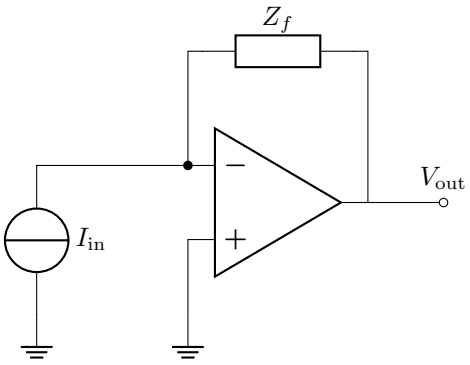

Figure 18: Basic transimpedance amplifier using voltage feedback operational amplifier.

The ideal operation amplifier has zero input current, thus, in the node of the inverting input of the operational amplifier Kirchhoff's law states that the current going through the feedback impedance has to cancel the current of the current source I_{in}. The current through the feedback impedance Z_f can be expressed in terms of the feedback impedance Z_f and the output voltage V_{out} of the operational amplifier through the use of Ohm's law, yielding,

$$V_{\text{out}} = -Z_f I_{\text{in}}. \tag{23}$$

Given a maximum current I_{in} and a desired maximum output voltage V_{out}, Equation (23) determines the feedback impedance. Limitations arise for real operational amplifiers where the output voltage is limited to be below the supply voltage of the operational amplifier.

Aside from photodiode applications, it is more common to find the inverting (voltage-to-voltage) operational amplifier in the literature. By using the source transformation on the current source with a parallel impedance in the transimpedance amplifier circuit, we can recover the inverting operational amplifier circuit, and thereby easily use results obtained for the inverting amplifier design.

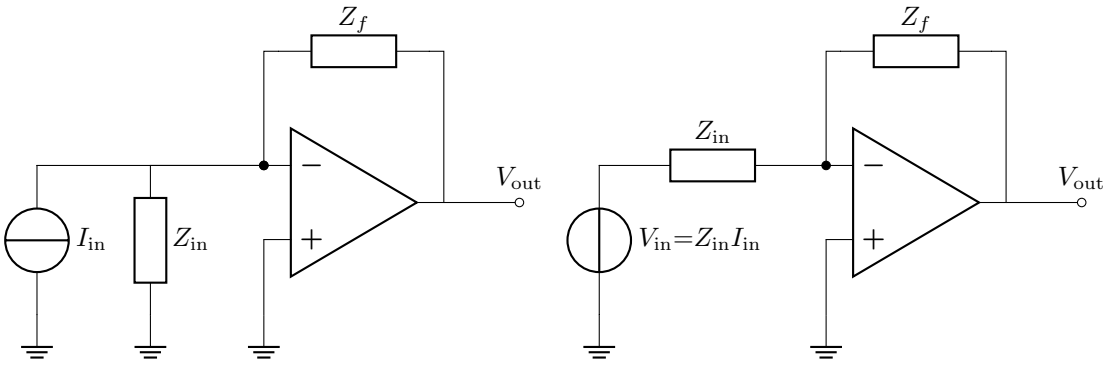

(a) Transimpedance amplifier. (b) Inverting amplifier.

Figure 19: Equivalence between transimpedance and inverting amplifier using source transformation.

Figure 19 shows the source transformation applied to transimpedance and inverting amplifier circuits. Given a current source I_{in} with parallel impedance Z_{in} the equivalent voltage source has value $V_{\text{in}} = Z_{\text{in}}I_{\text{in}}$ with impedance Z_{in} in series.

B.2. Input offset voltage

Real operational amplifiers only reduce the voltage difference between the inverting and non-inverting input to a non-zero input offset voltage. For high-precision operational amplifiers, the input offset voltage is in the range of microvolts. We can model the input offset voltage as a voltage source at the non-inverting input of an ideal operational amplifier in our transimpedance circuit, as can be seen from Figure 20. In Figure 20 we amended the basic transimpedance circuit of Figure 18 by inserting a voltage source with the input offset voltage between the non-inverting input and ground.

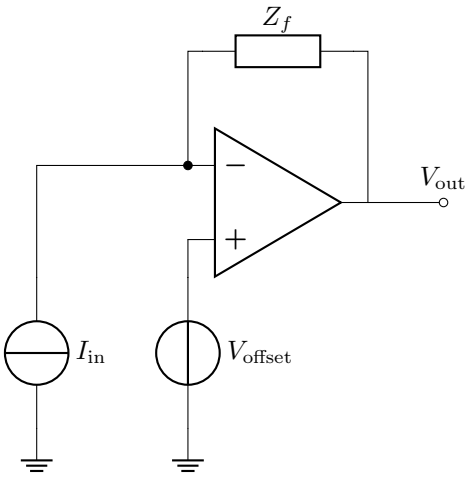

Figure 20: Input offset voltage in the transimpedance amplifier.

In order to estimate the output offset V_{out} caused by the input offset voltage V_{offset} we adapt the picture of the inverting amplifier. Figure 21 shows an inverting amplifier circuit with input impedance Z_{in} and input offset voltage V_{offset} at the non-inverting input of the operational amplifier. According to the superposition theorem, we can replace the input voltage source with a short circuit to estimate the contribution of the input offset voltage source.

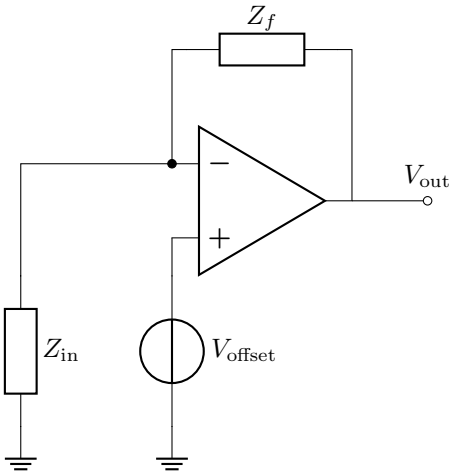

Figure 21: Input offset voltage in the inverting amplifier.

From Figure 21 we identify input and feedback impedance as a voltage divider in which

the input and output nodes are exchanged. The respective transfer function reads,

$$V_{\text{out}} = -\frac{R_f + R_{\text{in}}}{R_{\text{in}}} V_{\text{offset}} = -\left(1 + \frac{R_f}{R_{\text{in}}}\right) V_{\text{offset}}. \tag{24}$$

Comparing Equation (24) with Equation (23) discloses a difference in gain. The gain of the input signal in Eq. 1 is commonly referred to as signal gain. The gain of a signal applied directly to the inputs of the operational amplifier is referred to as noise gain. In the case of the position-sensitive detector, the input resistance is of order 10 kΩ. Using a feedback resistance of $R_f = 100\,\text{k}\Omega$ we find that the input offset voltage experiences a gain of 11.

One approach to compensate for the input offset voltage as described is depicted in Figure 22, see also Ref [**Jung05**]. A potentiometer with maximum resistance Rp connects the positive and negative supply voltage. The wiper of the potentiometer is connected with a first resistor R1 to a node. The node is connected with a second resistor R2 and an optional bypass capacitor to ground. Finally, the equivalent input offset voltage source connects the node with the non-inverting input of the operational amplifier.

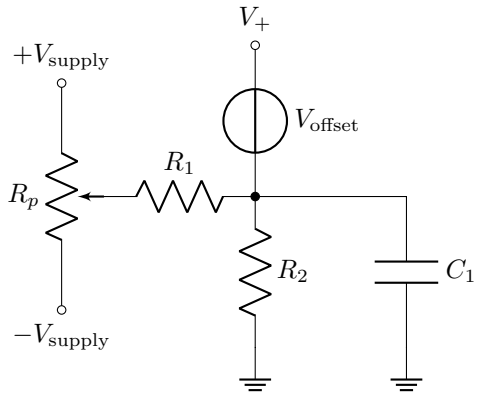

Figure 22: Input offset voltage compensation using adjustable potentiometer.

Let $0 \leq x \geq 1$ be the position of the potentiometer. For $x = 1/2$ the resistance of the potentiometer is $R_p/2$ and there is no offset compensation. For $x < 1/2$ the input offset compensation is negative to compensate for a positive input offset voltage. For $x > 1/2$ the input offset compensation is positive to compensate for a negative input offset voltage. The maximum input offset compensation is obtained for $x = 0$ and $x = 1$. Using circuit analysis techniques, we obtain,

$$V_c(x) = \frac{R_2(1-2x)}{R_1 + R_2 - R_p(1-x)x} V_{\text{supply}}, \tag{25}$$

as an analytical expression for the input offset voltage compensation measured between the node and ground. The maximum absolute value of the compensation voltage follows

to be,

$$V_c(0) = V_c(1) = \pm\frac{R_2}{R_1 + R_2} V_{\text{supply}}. \tag{26}$$

Given a maximum input offset voltage of 100 µV and a supply voltage of 15 V, we find approximate resistor values $R_1 = 3\,\text{M}\Omega$ and $R_2 = 2\,\Omega$. The resistor value of the potentiometer R_p should be chosen sufficiently large such to limit the current. For example, a potentiometer resistance of $R_p = 15\,\text{k}\Omega$ would limit the current to 2 mA with a heat dissipation of 60 mW. In practice, one should aim for a slightly higher maximum compensation voltage in order to handle resistor mismatches.

That said, there are some practical arguments against the use of the described input offset voltage compensation. The first argument is that the low resistance of R_2 acts as a dominant source for thermal current noise density of about $100\,\text{pA}/\sqrt{\text{Hz}}$. As this current noise contributes to the input of the transimpedance amplifier it gets amplified by the feedback impedance Z_f, yielding up to $110\,\mu\text{V}/\sqrt{\text{Hz}}$ in voltage noise density, which — depending on the bandwidth — surpasses the actual input offset voltage to compensate. The second argument is that high-precision potentiometers with large dynamic range get very large and difficult to accommodate on a printed circuit board.

B.3. Input bias current

In addition to the input offset voltage V_{offset}, there is a second effect that causes an offset in the output voltage V_{out}. This second effect stems from the small amount of current that is drawn from the inputs of the operational amplifier. We highlighted the input currents in Figure 23 where they are represented by the current flows i_+ and i_- directly pointing into the inputs of the operational amplifier in the transimpedance circuit.

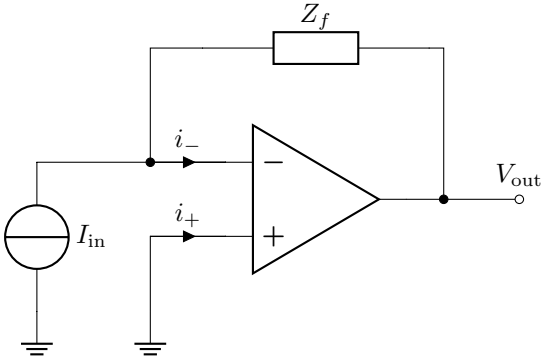

Figure 23: Input bias current offset in the transimpedance amplifier.

Input bias currents for high-precision operational amplifier are in the range of picoamperes. These small currents are usually difficult to measure and may differ between

inputs. The datasheet of the operational amplifier, therefore, doesn't report the input bias current per terminal but the mean I_{bias} and the difference between the input currents I_{offset}. The relationship between the mean input bias current I_{bias} and the input offset current I_{offset} with respect to the actual input bias currents i_+, i_- is given below.

$$i_+ = I_{\text{bias}} + \frac{1}{2} I_{\text{offset}} \qquad I_{\text{offset}} = i_+ - i_- \tag{27}$$

$$i_- = I_{\text{bias}} - \frac{1}{2} I_{\text{offset}} \qquad I_{\text{bias}} = \frac{i_+ + i_-}{2} \tag{28}$$

According to Ref. [**Jung05**] and Ref. [**Graeme96**] the effect of the input bias currents i_+, i_- on the output voltage V_{out} can be compensated with an impedance Z_c at the non-inverting input of the operational amplifier. Figure 24 illustrates the inverting amplifier configuration with such a compensation impedance Z_c.

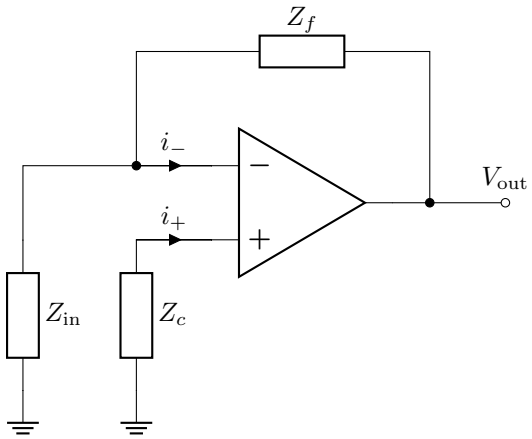

Figure 24: Input current offset compensation.

Following the argumentation from Ref. [**Terrel96**], the input bias current at the inverting input of the operational amplifier i_- develops a voltage of $Z_f i_-$ over the feedback impedance Z_f. The input bias current at the non-inverting input i_- develops the voltage $Z_c i_-$ over the compensation resistor Z_c. The voltage $Z_c i_-$ propagates through the voltage divider comprising the feedback and input impedance analogue to the input offset voltage. According to the superposition theorem, both of these contributions add and yield,

$$V_{\text{out}} = i_+ Z_c \left(1 + \frac{Z_f}{Z_{\text{in}}}\right) - i_- Z_f, \tag{29}$$

at the output voltage. If $i_+ \approx i_-$ we can choose,

$$Z_c = \frac{Z_{\text{in}}}{Z_{\text{in}} + Z_f}, \tag{30}$$

to compensate for the output voltage offset caused by the input bias currents. The condition $i_+ \approx i_-$ is usually satisfied if the input offset current I_{offset} reported in the

datasheet is less than the mean input bias current I_{bias}. High-precision operational amplifier usually have compensated bias currents that do not satisfy this condition. In this case, there is no generic formula for the value of the compensation impedance Z_c in terms of input and feedback impedance and one needs to perform impedance matching on a per-device basis. One should keep in mind that high-precision operational amplifier have input bias currents in the range of pA. Using Equation (29) one should therefore first check if the output voltage offset due to input bias currents is even worth compensating compared to other offset and noise contributions.

B.4. Stability and bandwidth

The outputs of the transimpedance and inverting amplifier designs have a phase shift of 180°. If an additional phase shift of 180° accumulates because of the inherent bandwidth limitations of the operational amplifier and the gain is equal or greater than unity, the conditions for oscillations are met and the amplifier will become unstable, see Ref. [**Terrel96**]. By artificially limiting the bandwidth with an additional frequency pole, we can flatten out the frequency response at high frequencies, and thereby stabilize the amplifier, see Ref. [**Kay12**].

Figure 25 shows a Bode plot of the open-loop (black) and noise gain (red) of an operational amplifier. The noise gain separates into a compensated (solid) and uncompensated (dotted) branch.

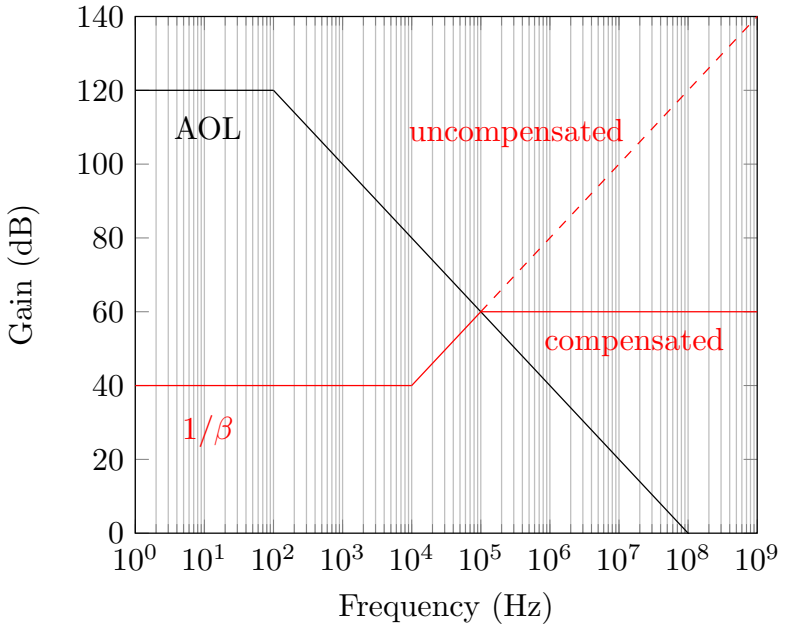

Figure 25: Bode plot of the open-loop and closed-loop gain of the amplifier.

With the uncompensated branch we would observe instability due to oscillations. The compensated branch is obtained through addition of a feedback capacitor. According to Ref. [**Jung05**], Ref. [**Hobbs11**] and Ref. [**Graeme96**] the value for the feedback capacitance is given by,

$$C_f \geq \sqrt{\frac{C_{\text{in}}}{2\pi R_f f_u}}, \tag{31}$$

wherein R_f denotes the feedback resistance and f_u the unity-gain-bandwidth of the operational amplifier. The capacitance should be chosen larger to ensure design margin. The unity-gain-bandwidth of the operational amplifier denotes the frequency where the open-loop gain equals unity and is reported in the datasheet as GBP of the operational amplifier. C_{in} in Equation (31) represents the sum of the input capacities of the amplifier circuit and the capacitance of the signal source. According to Ref. [**Carter17**] a more exact formula for the feedback capacitance is given by,

$$C_f \geq \frac{C_{\text{aux}}}{2}\left(1+\sqrt{1+\frac{4C_{\text{in}}}{C_{\text{aux}}}}\right) \qquad C_{\text{aux}} = \frac{1}{2\pi R_f f_u}, \tag{32}$$

which is also valid if not $C_{\text{in}} \gg C_f$.

Figure 26 illustrates the transimpedance amplifier with capacitive elements. Parallel to the current source I_{in} we find the input capacitance C_{in} comprising source capacitance

and operational amplifier capacitance. Parallel to the feedback resistance R_f we find the feedback capacitance C_f with value given in Equation (32) or Equation (31).

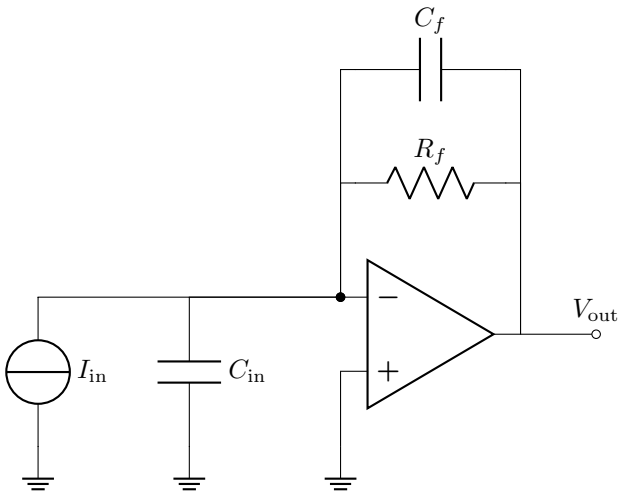

Figure 26: Transimpedance amplifier with capacitive elements.

As noted earlier, the bandwidth is reduced through the additional feedback capacitor. The new bandwidth is now given by the RC pole formed by the feedback impedance,

$$BW = \frac{1}{2\pi R_f C_f}. \tag{33}$$

Given a unity-gain-bandwidth of the operational amplifier of $f_u = 10\,\text{MHz}$ and a feedback resistance of $R_f = 100\,\text{k}\Omega$ Equation (31) yields a minimum feedback capacitance of $C_f = 4\,\text{pF}$. Together with R_f this feedback capacitance limits the bandwidth to about 400 kHz.

Glossary

BNC Bayonet Neill–Concelman. 16

BOM bill of materials. 11, 13

GBP gain-bandwidth-product. 7, 37

HTML hypertext markup language. 11–13

IC integrated circuit. 14

PCB printed circuit board. 7, 11, 13

PSD position-sensitive detector. 16

S5990 Hamamatsu two-dimensional PSD. 26

SMA SubMiniature version A. 13, 16

SMD surface mounted device. 13